We are IntechOpen, the world's leading publisher of Open Access books
Built by scientists, for scientists

6,900
Open access books available

186,000
International authors and editors

200M
Downloads

154
Countries delivered to

Our authors are among the

TOP 1%
most cited scientists

12.2%
Contributors from top 500 universities

CLARIVATE ANALYTICS
BOOK CITATION INDEX
INDEXED

WEB OF SCIENCE™

Selection of our books indexed in the Book Citation Index
in Web of Science™ Core Collection (BKCI)

Interested in publishing with us?
Contact book.department@intechopen.com

Numbers displayed above are based on latest data collected.
For more information visit www.intechopen.com

Modeling and Design of Plate Heat Exchanger

Fábio A.S. Mota, E.P. Carvalho and
Mauro A.S.S. Ravagnani

Additional information is available at the end of the chapter

1. Introduction

Heat exchangers are devices used to transfer energy between two fluids at different temperatures. They improve energy efficiency, because the energy already within the system can be transferred to another part of the process, instead of just being pumped out and wasted. In the new era of sustainability, the growing urgency to save energy and reduce overall environmental impacts has placed greater emphasis on the use of heat exchangers with better thermal efficiency. In this new scenario, the plate heat exchanger can play an important role.

A plate heat exchanger is a compact type of heat exchanger that uses a series of thin plates to transfer heat between two fluids. There are four main types of PHE: gasketed, brazed, welded, and semi-welded. The plate-and-frame or gasketed plate heat exchanger essentially consists of a pack of thin rectangular plates sealed around the edges by gaskets and held together in a frame (Figure 1). Plate heat exchangers were first introduced in 1923 for milk pasteurization applications, but are now used in many applications in the chemical, petroleum, HVAC, refrigeration, dairy, pharmaceutical, beverage, liquid food and health care sectors. This is due to the unique advantages of PHEs, such as flexible thermal design (plates can be simply added or removed to meet different heat duty or processing requirements), ease of cleaning to maintain strict hygiene conditions, good temperature control (necessary in cryogenic applications), and better heat transfer performance.

2. Mechanical characteristics

A PHE consists of a pack of thin rectangular plates with portholes, through which two fluid streams flow, where heat transfer takes place. Other components are a frame plate (fixed plate),

INTECH
open science | open minds

Figure 1. Typical plate heat exchangers [1].

a pressure plate (movable plate), upper and lower bars and screws for compressing the pack of plates (Figure 2). An individual plate heat exchanger can hold up to 700 plates. When the package of plates is compressed, the holes in the corners of the plates form continuous tunnels or manifolds through which fluids pass, traversing the plate pack and exiting the equipment. The spaces between the thin heat exchanger plates form narrow channels that are alternately traversed by hot and cold fluids, and provide little resistance to heat transfer.

2.1. Thermal plates and gaskets

The most important and most expensive part of a PHE is its thermal plates, which are made of metal, metal alloy, or even special graphite materials, depending on the application. Stainless steel, titanium, nickel, aluminum, incoloy, hastelloy, monel, and tantalum are some examples commonly found in industrial applications. The plates may be flat, but in most applications have corrugations that exert a strong influence on the thermal-hydraulic performance of the device. Some of the main types of plates are shown in Figure 3, although the majority of modern PHEs employ chevron plate types. The channels formed between adjacent plates impose a swirling motion to the fluids, as can be seen in Figure 4. The chevron angle is reversed in adjacent sheets, so that when the plates are tightened, the corrugations provide numerous points of contact that support the equipment. The sealing of the plates is achieved by gaskets fitted at their ends. The gaskets are typically molded elastomers, selected based on their fluid compatibility and conditions of temperature and pressure. Multi-pass arrangements can be implemented, depending on the arrangement of the gaskets between the plates. Butyl or nitrile rubbers are the materials generally used in the manufacture of the gaskets.
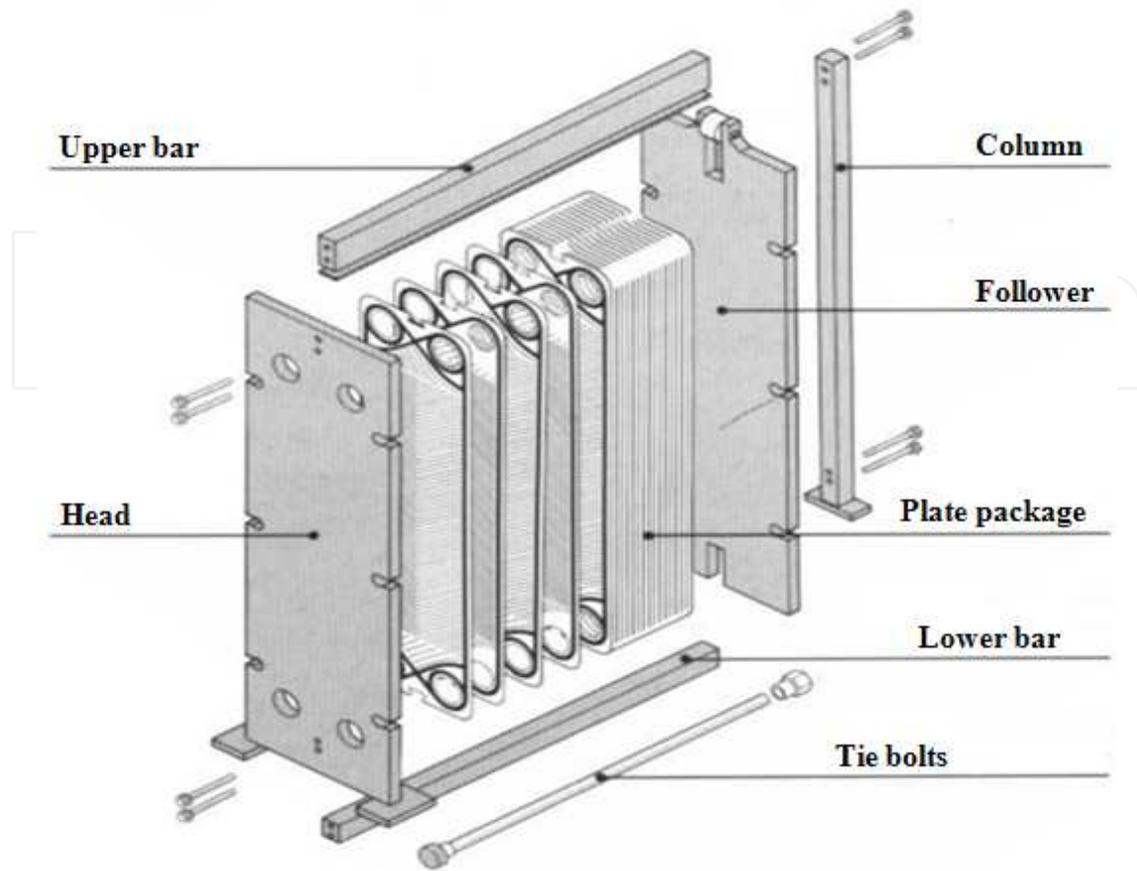
**Figure 2.** Exploded View of a Plate Heat Exchanger [2].
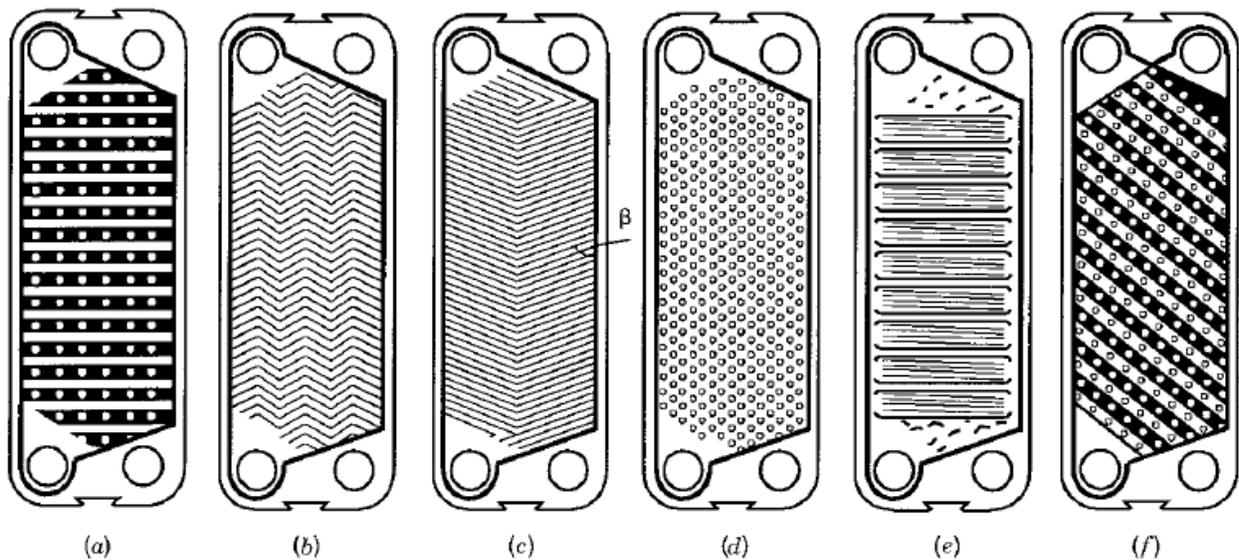
Figure 3. Typical cathegories of plate corrugations. (a) washboard, (b) zigzag, (c) chevron or herringbone, (d) protrusions and depressions (e) washboard with secondary corrugations, e (f) oblique washboard [3].
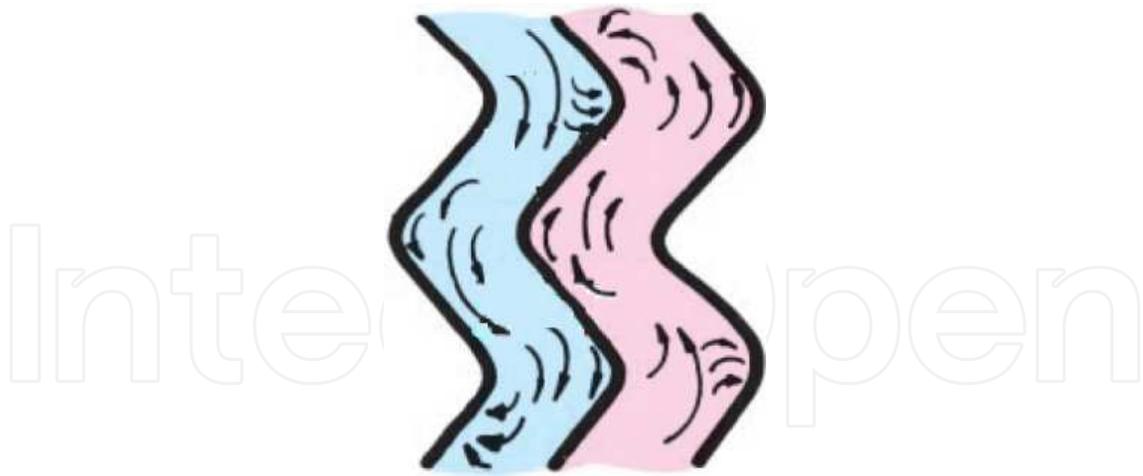
Figure 4. Turbulent flow in PHE channels [4].

2.2. Design characteristics

This section presents some of the main advantages and disadvantages of a PHE, compared to shell-and-tube heat exchangers.

Advantages

Flexibility: Simple disassembly enables the adaptation of PHEs to new process requirements by simply adding or removing plates, or rearranging the number of passes. Moreover, the variety of patterns of plate corrugations available, together with the possibility of using combinations of them in the same PHE, means that various conformations of the unit can be tested during optimization procedures.

Good temperature control: Due to the narrow channels formed between adjacent plates, only a small volume of fluid is contained in a PHE. The device therefore responds rapidly to changes in process conditions, with short lag times, so that the temperatures are readily controllable. This is important when high temperatures must be avoided. Furthermore, the shape of the channels reduces the possibility of stagnant zones (dead space) and areas of overheating.

Low manufacturing cost: As the plates are only pressed (or glued) together, rather than welded, PHE production can be relatively inexpensive. Special materials may be used to manufacture the plates in order to make them more resistant to corrosion and/or chemical reactions.

Efficient heat transfer: The corrugations of the plates and the small hydraulic diameter enhance the formation of turbulent flow, so that high rates of heat transfer can be obtained for the fluids. Consequently, up to 90% of the heat can be recovered, compared to only 50% in the case of shell-and-tube heat exchangers.

Compactness: The high thermal effectiveness of PHEs means that they have a very small footprint. For the same area of heat transfer, PHEs can often occupy 80% less floor space (sometimes 10 times less), compared to shell-and-tube heat exchangers (Figure 5).
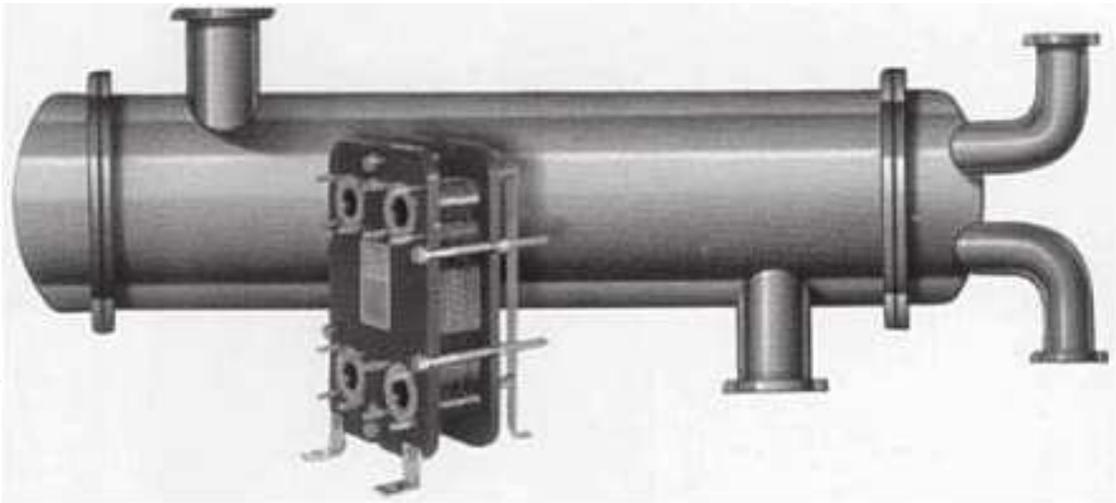
Figure 5. Illustration of the typical size difference between a PHE and a shell-and-tube heat exchanger for a given heat load [5].

Reduced fouling: Reduced fouling results from the combination of high turbulence and a short fluid residence time. The scale factors for PHEs can be up to ten times lower than for shell-and-tube heat exchangers.

Ease of inspection and cleaning: Since the PHE components can be separated, it is possible to clean and inspect all the parts that are exposed to fluids. This feature is essential in the food processing and pharmaceutical industries.

Easy leak detection: The gaskets have vents (Figure 6) that prevent fluids from mixing in the case of a failure, which also facilitate locating leaks.
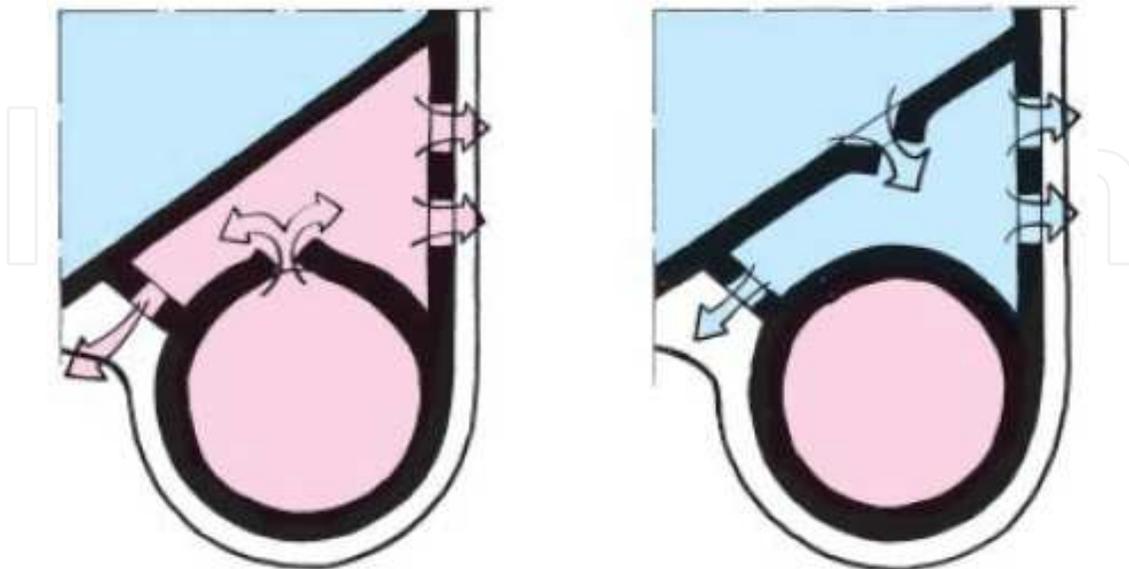

Figure 6. Vents in gaskets to detect possible leaks [4].

Drawbacks

Temperature and pressure limitations: An important limitation of PHEs is related to the plate gaskets. Pressures and temperatures exceeding 25 atm and 160 °C, respectively, are not tolerated because they can cause the standard gaskets to leak. However, gaskets made of special materials can withstand temperatures up to 400 °C, and it is possible to weld or braze the plates to each other in order to operate under more severe conditions. This would have the additional advantages of increasing the operational limits, as well as the possibility of working with corrosive fluids, because it would eliminate the need for gaskets. However, the PHE would lose its major advantages of flexibility and ease of cleaning, and the equipment would become more expensive.

High pressure drop: Because of the corrugated plates and the small flow space between them, the pressure drop due to friction is high, which increases pumping costs. The pressure drop can be reduced by increasing the number of passages per pass and splitting the flow into a greater number of channels. This diminishes the flow velocity within the channel, hence reducing the friction factor. However, the convective heat transfer coefficient is also reduced, decreasing the effectiveness of the heat exchanger.

Phase change: In special cases, PHEs can be used in condensation or evaporation operations, but are not recommended for gases and vapors due to the limited space within the channels and pressure limitations.

Types of fluids: The processing of fluids that are highly viscous or contain fibrous material is not recommended because of the high associated pressure drop and flow distribution problems within the PHE. Compatibility between the fluid and the gasket material should also be considered. Highly flammable or toxic fluids must be avoided due to the possibility of leakage.

Leakage: Friction between the metal plates can cause wear and the formation of small holes that are difficult to locate. As a precaution, it is advisable to pressurize the process fluid so that there is less risk of contamination in the event of leakage from a plate.

2.3. Arrangement of a plate heat exchanger

The simplest types of arrangements of plate heat exchangers are those in which both fluids make just one pass, so there is no change in direction of the streams. These are known as 1-1 single-pass arrangements, and there are two types: countercurrent and concurrent. A great advantage of the single-pass arrangement is that the fluid inlets and outlets can be installed in the fixed plate, making it easy to open the equipment for maintenance and cleaning, without disturbing the pipework. This is the most widely used single-pass design, known as the U-arrangement. There is also a single-pass Z-arrangement, where there is input and output of fluids through both end plates (Figure 7).

Countercurrent flow, where the streams flow in opposite directions, is usually preferred due the achievement of higher thermal efficiency, compared to concurrent flow, where the streams flow in the same direction. Multi-pass arrangements can also be employed to enhance the heat
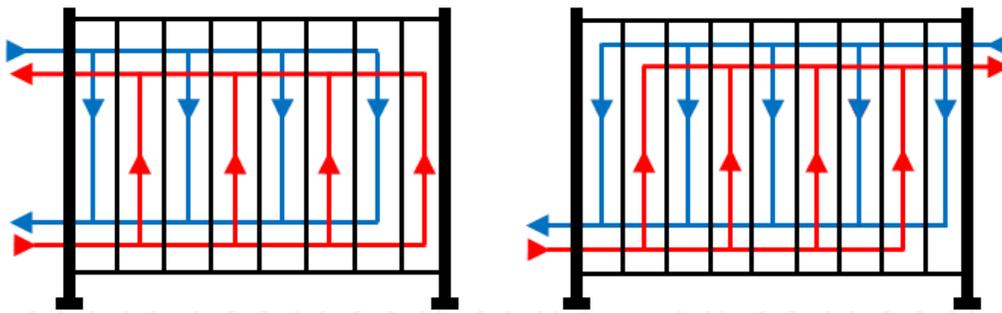
Figure 7. Arrangements of a simple-pass PHE. (a) U-arrangement and (b) Z-arrangement.

transfer or flow velocity of the streams, and are usually required when there is a substantial difference between the flow rates of the streams (Figure 8).
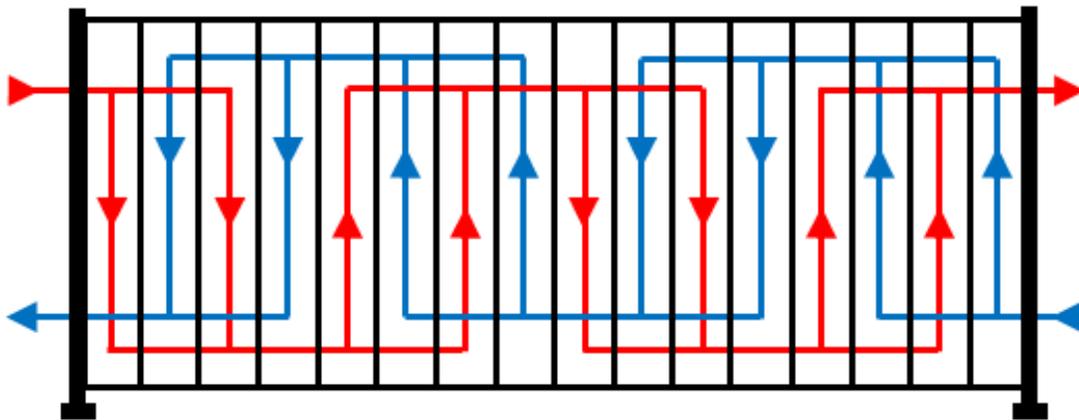

Figure 8. Multi-pass PHE.

There are five parameters that can be used to characterize the PHE configuration [6]: N_C, P^I, P^{II}, ϕ, Y_h and Y_f.

Number of channels (N_C): The space between two adjacent plates is a channel. The end plates are not considered, so the number of channels of a PHE is the number of plates minus one. The odd-numbered channels belong to side I, and the even-numbered ones belong to side II (Figure 9). The number of channels in each side are N_C^I and N_C^{II}.

Number of passes (P): This is the number of changes of direction of a determined stream inside the plate pack, plus one. P^I and P^{II} are the number of passes in each side.

Hot fluid location (Y_h): It is a binary parameter that assigns the fluids to the PHE sides. If Y_h = 1 the hot fluid occupies side I while if Y_h = 0 the hot fluid occupies side II.

Feed connection (ϕ): Feed side I is arbitrarily set at $\eta = 0$ as presented in Figure 9. The parameter ϕ represents the relative position of side II. Figure 9 illustrates all possibilities of connection. The parameter η is defined as $\eta = x / L_P$.
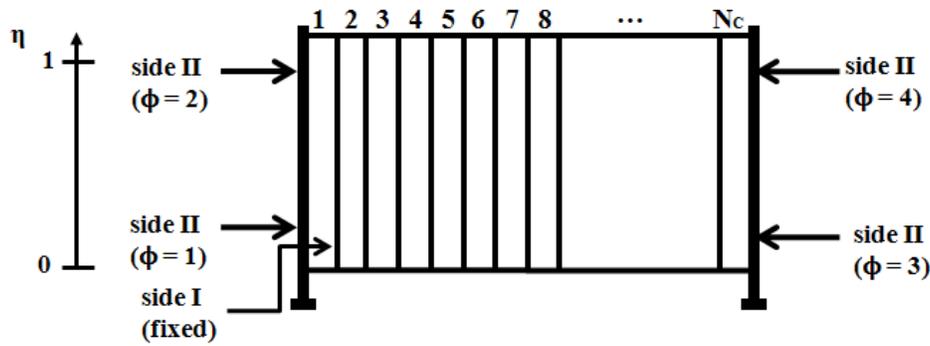
Figure 9. Feed connection of a PHE.

The plates of a PHE can provide vertical or diagonal flow, depending on the arrangement of the gaskets. For vertical flow, the inlet and outlet of a given stream are located on the same side of the heat exchanger, whereas for diagonal flow they are on opposite sides. Assembly of the plate pack involves alternating between the "A" and "B" plates for the respective flows. Mounting of the plate pack in vertical flow mode only requires an appropriate gasket configuration, because the A and B arrangements are equivalent (they are rotated by 180°, as shown in Figure 10a). This is not possible in the case of diagonal flow, which requires both types of mounting plate (Figure 10b). To identify each type of flow, Gut (2003) considered the binary parameter Y_f ($Y_f = 1$ for diagonal flow and $Y_f = 0$ for vertical flow). Poor flow distribution is more likely to occur in the array of vertical flow [7].


(a)

(b)
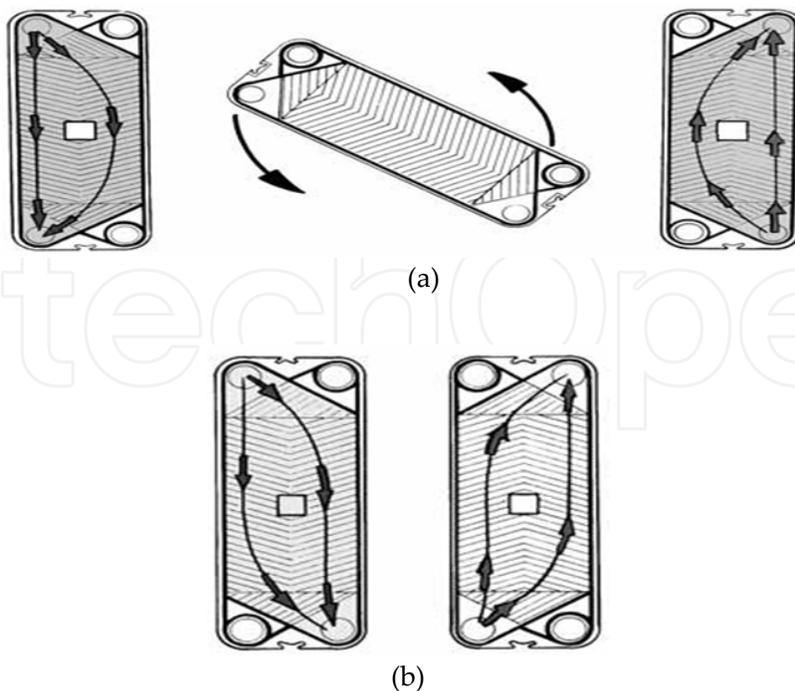
Figure 10. (a). Vertical flow plate [9]. (b). Diagonal flow plate [9].

3. Mathematical modeling

Due to the large number of plate types and pass arrangements, there are many possible configurations of a particular PHE design. As a result, a number of mathematical modeling approaches have been proposed for the calculation of performance. Two different modeling approaches are described below.

3.1. Model 1

A mathematical model was developed to simulate the general configuration of a PHE operating under steady state conditions, characterized using six different parameters [6]. In this model, the parameters considered are the number of channels, the number of passes for each side, the fluid locations, the feed connection locations, and the type of channel flow. The following assumptions are made:

- The PHE operates at steady state;

- The main flow is divided equally among the channels that make up each pass;

- The velocity profile in the channels is flat (plug flow);

- Perfect mixture in the end of each pass;

- There are no heat losses to the environment;

- There are no phase change;

- There is no heat transfer in the direction of flow, either in the fluids or in the plates, so heat transfer only occurs in the direction perpendicular to the flow;

- The physical properties of the fluids remain constant throughout the process.

The last assumption listed above implies an overall heat transfer coefficient U constant throughout the process, which is quite reasonable for compact heat exchangers operating without phase change [10]. In the absence of this consideration, the energy balance in the channels would result in a nonlinear system of ordinary first order differential equations, which would make the simulation much more complex. It has also been found that the results obtained assuming a constant overall heat transfer coefficient are very close to those found without such a restriction [6]. Thus, this assumption is not a limiting factor for the evaluation of a PHE.

Applying the energy conservation law to a given volume of control of a generic channel i with dimensions W_P, δx and b (Figure 11) and neglecting variations of kinetic and potential energy, the enthalpy change of the fluid passing through the volume is equal to the net heat exchanged by the two adjacent channels. This can be described by a system of differential equations:

$$\frac{d\theta_1}{d\eta} = s_1 \alpha^I \left(\theta_2 - \theta_1 \right) \tag{1}$$
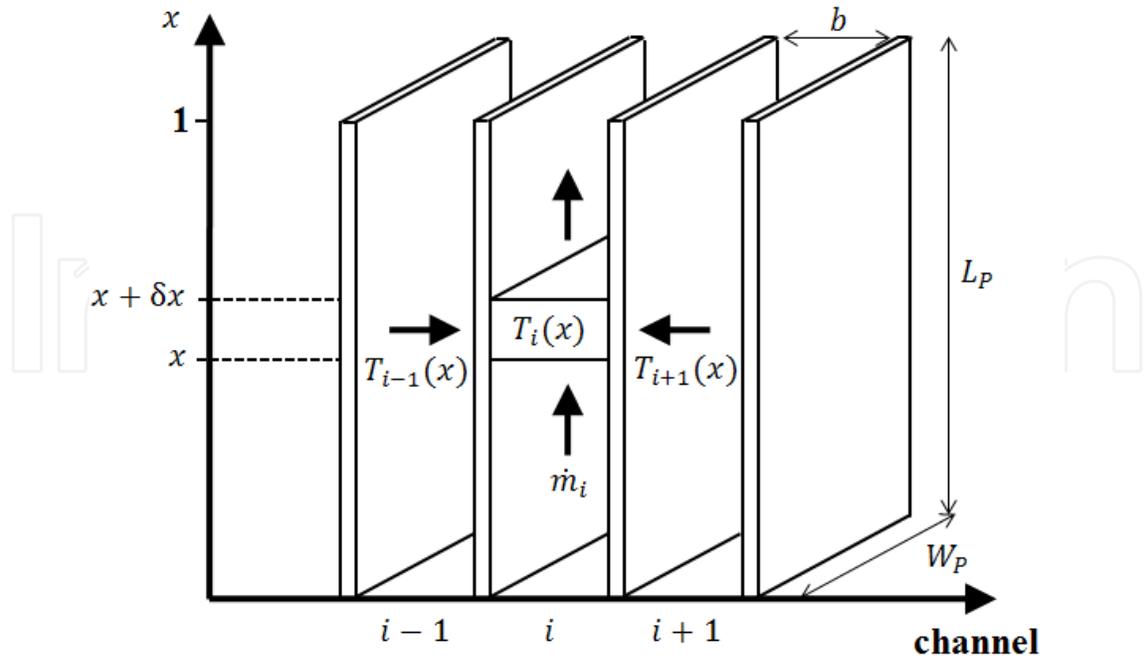
Figure 11. Scheme of a fluid control volume

$$\frac{d\theta_1}{d\eta} = s_i \alpha^{side(i)} \left(\theta_{i-1} + 2\theta_i + \theta_{i+1} \right) side(i) = \{I, II\} \tag{2}$$

$$\frac{d\theta_1}{d\eta} = s_i \alpha^{side(N_C)} \left(\theta_{N_c-1} - \theta_{N_c} \right) side(N_C) = \{I, II\} \tag{3}$$

where s_i is a constant that represents the flow direction in the channels (s = 1 for upward flow and s = - 1 for downward flow); θ is the adimensional temperature:

$$\theta = \frac{T_i - T_{cold,in}}{T_{hot,in} - T_{cold,in}} \tag{4}$$

and

$$\alpha^I = \frac{A_p U N^I}{\dot{M}^I c_p^{\,I}}, \quad \alpha^{II} = \frac{A_p U N^{II}}{\dot{M}^{II} c_p^{\,II}} \tag{5}$$

A_p is the plate area, U is the overall heat transfer coefficient, N is the number of channels per pass, $\dot{M}$ is the mass flow and c_p is the specific heat.

This system of linear differential equations can be written in the matrix form as:

$$\frac{d\bar{\theta}}{d\eta} = \bar{\bar{M}}.\bar{\theta} \tag{6}$$

where

$$\bar{\bar{M}} = \begin{bmatrix} -d_1 & +d_1 & 0 & & 0 & \cdots & 0 \\ +d_2 & -2d_2 & +d_2 & & 0 & \cdots & 0 \\ 0 & +d_3 & -2d_3 & & +d_3 & & \vdots \\ \vdots & & & & & & 0 \\ 0 & \cdots & 0 & +d_{N_C-1} & -2d_{N_C-1} & +d_{N_C-1} \\ 0 & \cdots & 0 & 0 & +d_{N_C} & -d_{N_C} \end{bmatrix}$$

$$d_i = \begin{cases} s_i \alpha^I & [\ \text{if } i \text{ is odd} \\ s_i \alpha^{II} & \text{if } i \text{ is even} \end{cases} i = 1,...,N_C$$

The boundary conditions, which are dependent on the PHE configuration, can be divided into three different categories:

1. *Fluid inlet temperature*: In the channels of the first pass, the fluid inlet temperature is the fluid feed temperature.

$$\theta_i(\eta) = \theta_{fluid,in} i \ \epsilon \ \text{first pass} \tag{7}$$

2. *Change of pass temperature*: The temperature at the beginning of the channels of a particular pass is equal to the arithmetic average of the temperatures in the channels of the previous pass.

$$\theta_i(\eta) = \frac{1}{N} \sum_{\substack{j\,\epsilon\,previous\\pass}}^{N} \theta_j(\eta)\ i\ \epsilon\ \text{new pass} \tag{8}$$

3. *Fluid outlet temperature*: The outlet temperature of the fluid is the arithmetic average of the outlet temperatures of the channels of the last pass.

$$\theta_{fluid,out}(\eta) = \frac{1}{N} \sum_{\substack{j\,\epsilon\,last\\pass}}^{N} \theta_j(\eta) \tag{9}$$

The analytical solution is given by Eq. (10), where λ_i and $\bar{z}_i$ are, respectively, the eigenvalues and eigenvectors of matrix $\overline{\overline{M}}$:

$$\bar{\theta}(\eta) = \sum_{i=1}^{N_c} c_i \bar{z}_i e^{\lambda_i \eta} \tag{10}$$

Application of Eq. (10) in the boundary condition equations for the fluid inlet and change of pass enables the creation of a linear system of N_c equations for c_i variables. After solving the linear system, the outlet temperatures can be determined by the use of the outlet boundary conditions, hence enabling the thermal effectiveness to be determined.

Example: Creation of the linear system of N_c equations:

In order to illustrate the generation of the linear system, a PHE containing 7 thermal plates (or 8 channels), with the cold fluid making two passes and the hot fluid making one pass, is shown in Figure 12.
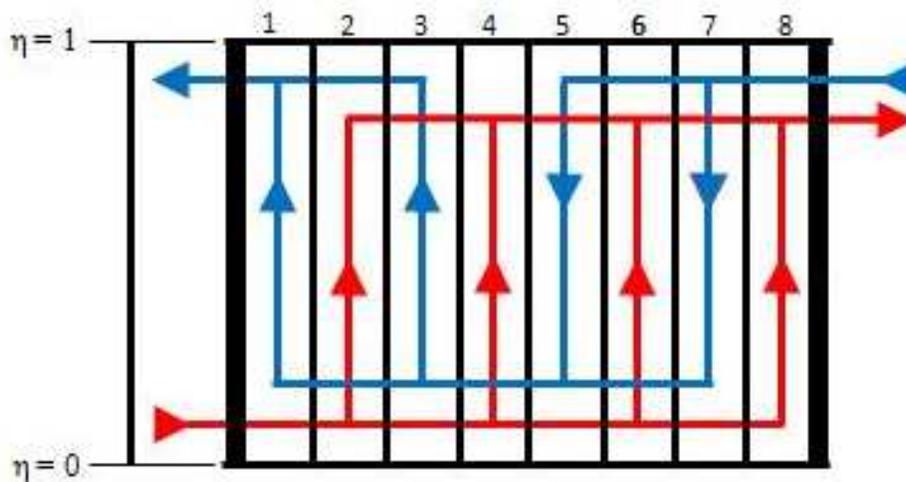
Figure 12. PHE streams.

Applying Eq. (10), the following analytical solution can be achieved:

$$\bar{\theta}(\eta) = c_1 \begin{bmatrix} z_{1,1} \\ z_{2,1} \\ \vdots \\ z_{8,1} \end{bmatrix} e^{\lambda_1 \eta} + c_2 \begin{bmatrix} z_{1,2} \\ z_{2,2} \\ \vdots \\ z_{8,2} \end{bmatrix} e^{\lambda_2 \eta} + \dots + c_8 \begin{bmatrix} z_{1,8} \\ z_{2,8} \\ \vdots \\ z_{8,8} \end{bmatrix} e^{\lambda_8 \eta}$$

Using the boundary condition equations (7) and (8) for all the channels of the PHE under investigation, the equations presented in Table 1 are generated.

Cold fluid	Hot fluid
$\theta_1(\eta=0)=[\theta_5(\eta=0)+\theta_7(\eta=0)]/2$	$\theta_2(\eta=1)=\theta_{hot,in}=1$
$\theta_3(\eta=0)=[\theta_5(\eta=0)+\theta_7(\eta=0)]/2$	$\theta_4(\eta=1)=\theta_{hot,in}=1$
$\theta_5(\eta=1)=\theta_{cold,in}=0$	$\theta_6(\eta=1)=\theta_{hot,in}=1$
$\theta_7(\eta=1)=\theta_{cold,in}=0$	$\theta_8(\eta=1)=\theta_{hot,in}=1$

Table 1. Boundary condition equations.

These equations can be written in the following way:

$$\theta_1\left(\eta=0\right)-\left[\theta_5\left(\eta=0\right)+\theta_7\left(\eta=0\right)\right]/2=0$$
$$\theta_2\left(\eta=1\right)=1$$
$$\theta_3\left(\eta=0\right)-\left[\theta_5\left(\eta=0\right)+\theta_7\left(\eta=0\right)\right]/2=0$$
$$\theta_4\left(\eta=1\right)=1$$
$$\theta_5\left(\eta=1\right)=0$$
$$\theta_6\left(\eta=1\right)=1$$
$$\theta_7\left(\eta=1\right)=0$$
$$\theta_8\left(\eta=1\right)=1$$

To achieve the matrix form is Eq. (10) is applied to the linear system:

$$\overline{\overline{A}}.\overline{C}=\overline{B} \tag{11}$$

where

$\overline{\overline{A}}=$ eigenvalues and eigenvectors matrix

$\overline{C}=c_i'$ s coefficients vector

$\overline{B}=$ binary vector

where

$$B_i=0 \text{ if } B_i=\theta_{hot,in} \; i \in \text{first pass}$$
$$B_i=1 \text{ if } B_i=\theta_{cold,in} \; i \in \text{first pass}$$
$$B_i=0 \text{ if } B_i=\theta_i(\eta)-\frac{1}{N}\sum_{j \in previous\; pass}^{N}\theta_j(\eta)$$

3.2. Model 2

The assumption is made that any multi-pass PHE with a sufficiently large number of plates (so that end effects and inter-pass plates can be neglected) can be reduced to an arrangement consisting of assemblies of single-pass PHEs [11]. This enables the development of closed-form equations for effectiveness, as a function of the ratio between the heat capacities of the fluids and the number of transfer units, for the arrangements 1-1, 2-1, 2-2, 3-1, 3-2, 3-3, 4-1, 4-2, 4-3, and 4-4 (Table 2). In other words, most multi-pass plate heat exchangers can be represented by simple combinations of pure countercurrent and concurrent exchangers, so that a multi-pass PHE is therefore equivalent to combinations of smaller single-pass exchangers (Figure 13).
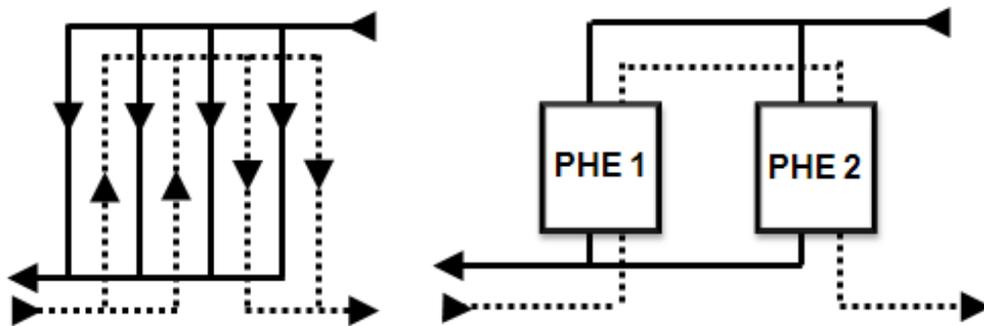
Figure 13. Equivalent configurations.

The assumptions considered are the same as in the first mathematical model. The derived formulas are only valid for PHEs with numbers of thermal plates sufficiently large that the end effects can be neglected. This condition can be satisfied, depending on the required degree of accuracy. For example, a minimum of 19 plates is recommended for an inaccuracy of up to 2.5% [12]. Elsewhere, a minimum of 40 thermal plates was used [11, 13]. In the formulas, P_{CC} and P_P are the thermal effectiveness for the countercurrent and concurrent flows, respectively, given by:

$$P_{CC}\left(NTU_1, R_1\right) = \begin{cases} \dfrac{1 - e^{-NTU_1\left(1-R_1\right)}}{1 - R_1 e^{-NTU_1\left(1-R_1\right)}} & se \, R_1 \neq 1 \\[4mm] \dfrac{NTU_1}{NTU_1 + 1} & se \, R_1 = 1 \end{cases} \tag{12}$$

$$P_P\left(NTU_1, R_1\right) = \frac{1 - e^{-NTU_1\left(1+R_1\right)}}{1 + R_1} \tag{13}$$

Formulas	Arrangements
Arrangement 111 $P_1 = P_{CC}$ where: $P_{CC} = P_{CC}(NTU_1, R_1)$	
Arrangement 211 $P_1 = \frac{1}{2}\left[P_{CC} + P_P - \frac{1}{2}(P_P P_{CC} R_1)\right]$ where: $P_{CC} = P_{CC}(NTU_1, R_1)$ $P_P = P_P(NTU_1, R_1/2)$	
Arrangement 221 $P_1 = P_{CC}$ where: $P_{CC} = P_{CC}(NTU_1, R_1)$	
Arrangement 311 $P_1 = \frac{1}{3}\left[P_{B,1} + P_{A,1}\left(1 - \frac{P_{B,1}R_1}{3}\right)\left(2 - \frac{P_{A,1}R_1}{3}\right)\right]$ where: $P_{A,1} = P_{CC}$ $P_{B,1} = P_P$ $P_{CC} = P_{CC}(NTU_1, R_1/3)$ $P_P = P_P(NTU_1, R_1/3)$	
Arrangement 321 $P_1 = \frac{1}{R_1}(a + 0,5b + 0,5c + d)$ where: $a = \dfrac{2R_1 ef^2 - 2ef - f^2}{2R_1 e^2 f^2 - e^2 - f^2 - 2ef + e + f}$ $b = \dfrac{a(e-1)}{f}$, $c = \dfrac{(1-a)}{e}$ $d = R_1 e^2 c - R_1 e + R_1 - c/2$ $e = \dfrac{1}{(\frac{2}{3}R_1 P_{CC})}$, $f = \dfrac{1}{(\frac{2}{3}R_1 P_P)}$ $P_{CC} = P_{CC}(NTU_1/2, 2R_1/3)$ $P_P = P_P(NTU_1/2, 2R_1/3)$	
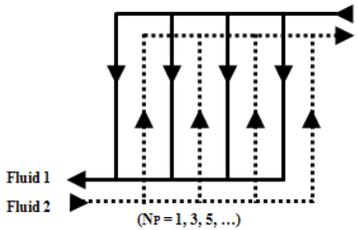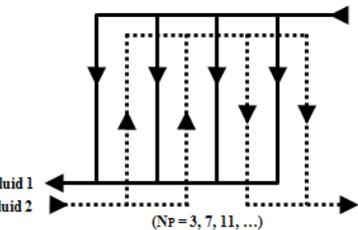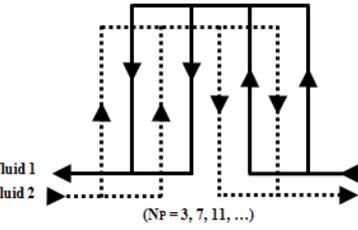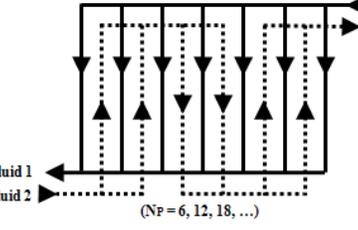
Formulas	Arrangements
Arrangement 331 $P_1 = P_{CC}$ where: $P_{CC} = P_{CC}(NTU_1, R_1)$	 Fluid 1 Fluid 2 (NP = 5, 11, 17, …)
Arrangement 411 $P_1 = P_I - \dfrac{P_I{}^2 R_1}{4}$ where: $P_I = \dfrac{1}{2}\left(P_{CC} + P_P - \dfrac{R_1 P_{CC} P_P}{4}\right)$ $P_{CC} = P_{CC}(NTU_1, R_1/4)$ $P_P = P_P(NTU_1, R_1/4)$	 Fluid 1 Fluid 2 (NP = 7, 15, 23, …)
Arrangement 421 $P_1 = P_I - \dfrac{P_I(1-P_I)(1-P_I R_1)}{1-P_I{}^2 R_1}$ where: $P_I = \dfrac{1}{2}\left(P_{CC} + P_P - \dfrac{P_{CC} P_P R_1}{2}\right)$ $P_{CC} = P_{CC}(NTU_1/2, R_1/2)$ $P_P = P_P(NTU_1/2, R_1/2)$	 Fluid 1 Fluid 2 (NP = 7, 15, 23, …)
Arrangement 431 $P_1 = A + \dfrac{\left[BD(1-G) + BQE\right]}{\left[(1-G)(1-E) - QS\right]}$ where: $A = \dfrac{1}{4}(3P_{CC} + P_P - rP_{CC}P_P)$ $B = 1 - A$	 Fluid 1 Fluid 2 (NP = 6, 16, 23, …)
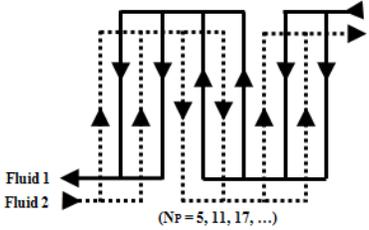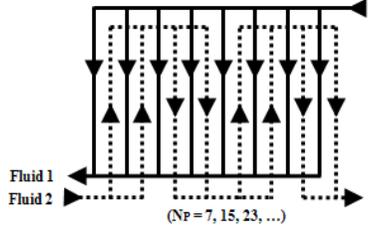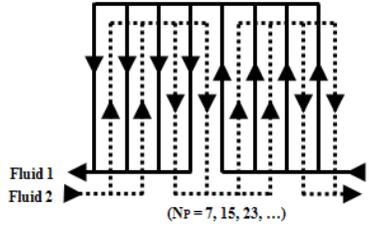
$D = \dfrac{1}{6}(1 - rP_{CC})(3P_{CC} + 3P_P - 2rP_{CC}P_P - rP_P{}^2)$

$E = \dfrac{1}{12}(1 - rP_{CC})(3 - 2rP_{CC} - rP_P)(P_{CC} + 3P_P - rP_{CC}P_P - 2rP_P{}^2)$

$G = \dfrac{r}{6}[(P_{CC}{}^2 + 3P_P{}^2) + P_{CC}P_P(3 - rP_{CC} - 2rP_P)]$

$H = \dfrac{r}{6}[3P_{CC}{}^2 + P_P{}^2 + P_{CC}P_P(3 - 2rP_{CC} - rP_P)]$

$Q = 1 - \dfrac{(P_{CC} + P_P)}{2} + \dfrac{rP_{CC}P_P}{3}$

$S = \dfrac{ErP_{CC}}{1 - rP_{CC}} + \dfrac{rP_P}{12}(P_{CC} + 3P_P - rP_P(P_{CC} + 2P_P))$

$r = \dfrac{3R_1}{4}$

$P_{CC} = P_{CC}(NTU_1/3, r)$

$P_P = P_P(NTU_1/3, r)$
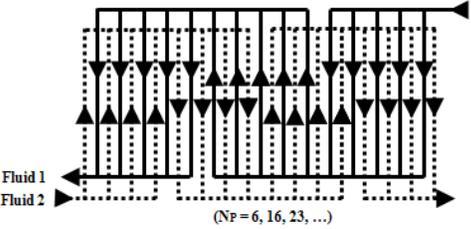
Formulas	Arrangements
Arrangement 441 $P_1 = P_{CC}$ where: $P_{CC} = P_{CC}(NTU_1, R_1)$	
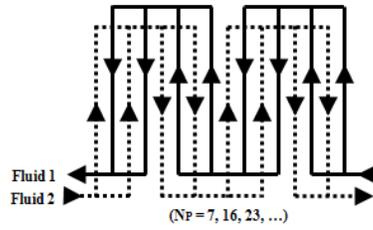
Table 2. Closed formulas for multi-pass arrangement [11]

4. Design of a plate heat exchanger

4.1. Basic equations for the design of a plate heat exchanger

The methodology employed for the design of a PHE is the same as for the design of a tubular heat exchanger. The equations given in the present chapter are appropriate for the chevron type plates that are used in most industrial applications.

4.1.1. Parameters of a chevron plate

The main dimensions of a *chevron* plate are shown in Figure 14. The corrugation angle, β, usually varies between extremes of 25° and 65° and is largely responsible for the pressure drop and heat transfer in the channels.
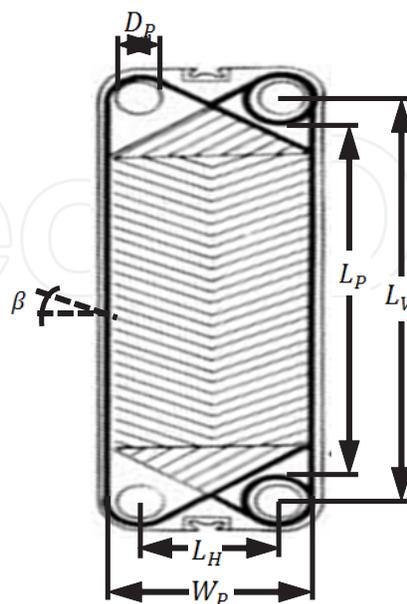
Figure 14. Parameters of a chevron plate.

The corrugations must be taken into account in calculating the total heat transfer area of a plate (effective heat transfer area):

$$A_p = \Phi.W_P.L_P \tag{14}$$

where

A_P = plate effective heat transfer area

Φ = plate area enlargement factor (range between 1.15 and 1.25)

W_P = plate width

L_P = plate length

The enlargement factor of the plate is the ratio between the plate effective heat transfer area, A_P and the designed area (product of length and width $W_P.L_P$), and lies between 1.15 and 1.25. The plate length L_P and the plate width W_P can be estimated by the orifices distances. L_V, L_H, and the port diameter D_p are given by Eq. (15) and Eq. (16) [5].

$$L_P \approx L_V - D_p \tag{15}$$

$$W_P \approx L_H + D_p \tag{16}$$

For the effective heat transfer area, the hydraulic diameter of the channel is given by the equivalent diameter, D_e, which is given by:

$$D_e = \frac{2b}{\Phi} \tag{17}$$

where b is the channel average thickness.

4.1.2. Heat transfer in the plates

The heat transfer area is expressed as the global design equation:

$$Q = UA\Delta T_M \tag{18}$$

where U is the overall heat transfer coefficient, A is the total area of heat transfer and ΔT_M is the effective mean temperature difference, which is a function of the inlet and outlet fluid

temperatures, the specific heat, and the configuration of the exchanger. The total area of heat transfer can be given by:

$$A = N_P A_P \tag{19}$$

where N_P is the number of plates. The end plates, which do not exchange heat, are not taken into account in determining the area. The inner plates are usually called thermal plates in order to distinguish them from the adiabatic end plates. The overall heat transfer coefficient can be determined by:

$$U = \frac{1}{\dfrac{1}{h_{hot}} + \dfrac{t_P}{k_P} + \dfrac{1}{h_{cold}} + R_{f,cold} + R_{f,hot}} \tag{20}$$

where

h_{hot} = convective heat transfer coefficient of the hot fluid

h_{cold} = convective heat transfer coefficient of the cold fluid

t_P = plate thickness

k_P = plate thermal conductivity

$R_{f,hot}$ = fouling factor of the hot fluid

$R_{f,cold}$ = fouling factor of the cold fluid

The convective heat transfer coefficient, h, depends on the fluid properties, fluid velocity, and plate geometry.

4.1.3. Design methods

There are two main approaches used in the design of PHEs, namely the log-mean temperature difference and the thermal effectiveness methods. For the first method, the rate of heat transfer is given by:

$$Q = UA(F\Delta T_{lm}) \tag{21}$$

where ΔT_{lm} is the log-mean temperature difference, given by Eq. (22) and F is the log-mean temperature difference correction factor.

$$\Delta T_{lm} = \frac{\Delta T_1 - \Delta T_2}{ln\left(\Delta T_1 / \Delta T_2\right)} \tag{22}$$

Where

$$\Delta T_1 = \begin{cases} T_{hot,in} - T_{cold,out} & \text{if countercurrent} \\ T_{hot,in} - T_{cold,in} & \text{if concurrent} \end{cases}$$

$$\Delta T_2 = \begin{cases} T_{hot,out} - T_{cold,in} & \text{if countercurrent} \\ T_{hot,out} - T_{cold,out} & \text{if concurrent} \end{cases}$$

The correction factor is a function of the heat exchanger configuration and the dimensionless parameters R and P_C. For purely countercurrent or concurrent (single-pass) arrangements, the correction factor is equal to one, while for multi-pass arrangements, it is always less than one. However, because the end channels of the PHE only exchange heat with one adjacent channel, different to the inner channels that exchange heat with two adjacent channels, purely countercurrent or concurrent flow is only achieved in two extreme situations. These are:

i.   when the PHE has only one thermal plate, so that only two channels are formed by the end plates and the thermal plate, with each stream flowing through one channel;

ii.   when the number of thermal plates is sufficiently large that the edge effect can be neglected.

The adimensional parameters R e P_C are defined as:

$$R = \frac{T_{hot,in} - T_{hot,out}}{T_{cold,out} - T_{cold,in}} = \frac{(\dot{M}c_p)_{cold}}{(\dot{M}c_p)_{hot}} \tag{23}$$

$$P_C = \frac{T_{cold,out} - T_{cold,in}}{T_{hot,in} - T_{cold,in}} = \frac{\Delta T_{cold}}{\Delta T_{max}} \tag{24}$$

The second method provides a definition of heat exchanger effectiveness in terms of the ratio between the actual heat transfer and the maximum possible heat transfer, as shown in Eq. (25):

$$E = \frac{Q}{Q_{max}} \tag{25}$$

The actual heat transfer can be achieved by an energy balance:

$$Q = \left(\dot{M}c_p\right)_{hot}\left(T_{hot,in} - T_{hot,out}\right) \tag{26}$$

$$Q = \left(\dot{M}c_p \right)_{cold} \left(T_{cold,out} - T_{cold,in} \right) \tag{27}$$

Thermodynamically, Q_{max} represents the heat transfer that would be obtained in a pure countercurrent heat exchanger with infinite area. This can be expressed by:

$$Q_{max} = \left(\dot{M}c_p \right)_{min} \Delta T_{max} \tag{28}$$

Using Eqs. (26), (27) and (28), the PHE effectiveness can be calculated as the ratio of temperatures:

$$E = \begin{cases} \dfrac{\Delta T_{hot}}{\Delta T_{max}} & \text{if } R > 1 \\[2ex] \dfrac{\Delta T_{cold}}{\Delta T_{max}} & \text{if } R < 1 \end{cases} \tag{29}$$

The effectiveness depends on the PHE configuration, the heat capacity rate ratio (R), and the number of transfer units (NTU). The NTU is a dimensionless parameter that can be considered as a factor for the size of the heat exchanger, defined as:

$$NTU = \frac{UA}{(\dot{M}c_p)_{min}} \tag{30}$$

4.1.4. Pressure drop in a plate heat exchanger

The pressure drop is an important parameter that needs to be considered in the design and optimization of a plate heat exchanger. In any process, it should be kept as close as possible to the design value, with a tolerance range established according to the available pumping power. In a PHE, the pressure drop is the sum of three contributions:

1. Pressure drop across the channels of the corrugated plates.

2. Pressure drop due to the elevation change (due to gravity).

3. Pressure drop associated with the distribution ducts.

The pressure drop in the manifolds and ports should be kept as low as possible, because it is a waste of energy, has no influence on the heat transfer process, and can decrease the uniformity of the flow distribution in the channels. It is recommended to keep this loss lower than 10% of the available pressure drop, although in some cases it can exceed 30% [3].

$$\Delta P = \frac{2fL_V P G_C^2}{\rho D_e} + 1,4 \frac{G_P^2}{2\rho} + \rho g L_V \tag{31}$$

where f is the Fanning fator, given by Eq. (33), P is the number of passes and G_P is the fluid mass velocity in the port, given by the ratio of the mass flow, $\dot{M}$, and the flow cross-sectional area, $\pi D_P{}^2/4$.

$$G_P = \frac{4\dot{M}}{\pi D_P{}^2} \tag{32}$$

$$f = \frac{K_p}{Re^m} \tag{33}$$

The values for K_p and m are presented in Table 3 as function of the Reynolds number for some β values.

4.1.5. Experimental heat transfer and friction correlations for the chevron plate PHE

Due to the wide range of plate designs, there are various parameters and correlations available for calculations of heat transfer and pressure drop. Despite extensive research, there is still no generalized model. There are only certain specific correlations for features such as flow patterns, parameters of the plates, and fluid viscosity, with each correlation being limited to its application range. In this chapter, the correlation described in [14] was used.

$$Nu = C_h(Re)^n (Pr)^{1/3} \left(\frac{\mu}{\mu_w}\right)^{0,17} \tag{34}$$

where μ_w is the viscosity evaluated at the wall temperature and the dimensionless parameters Nusselt number (Nu), Reynolds number (Re) and Prandtl number (Pr) can be defined as:

$$Nu = \frac{hD_e}{k} \ , \ Re = \frac{G_C D_e}{\mu} \ , \ Pr = \frac{c_p \mu}{k} \tag{35}$$

In Reynolds number equation, G_C is the mass flow per channel and may be defined as the ratio between the mass velocity per channel $\dot{m}$ and the cross sectional area of the flow channel (bW_P):

$$G_C = \frac{\dot{m}}{bW_P} \tag{36}$$

The constants C_h and n, which depend on the flow characteristics and the chevron angle, are given in Table 3.

4.2. Optimization

Any industrial process, whether at the project level or at the operational level, has aspects that can be enhanced. In general, the optimization of an industrial process aims to increase profits and/or minimize costs. Heat exchangers are designed for different applications, so there can be multiple optimization criteria, such as minimum initial and operational costs, minimum volume or area of heat transfer, and minimum weight (important for space applications).

β	Heat transfer			Pressure drop		
	Re	C_h	n	Re	K_p	m
≤ 30°	≤ 10	0.718	0.349	≤ 10	50.000	1.000
	> 10	0.348	0.663	10 - 100	19.400	0.589
				> 100	2.990	0.183
45 °	< 10	0.718	0.349	< 15	47.000	1.000
	10 - 100	0.400	0.598	15 - 300	18.290	0.652
	> 100	0.300	0.663	> 300	1.441	0.206
50 °	< 20	0.630	0.333	< 20	34.000	1.000
	20 - 300	0.291	0.591	20 - 300	11.250	0.631
	> 300	0.130	0.732	> 300	0.772	0.161
60 °	< 20	0.562	0.326	< 40	24.000	1.000
	20 - 200	0.306	0.529	40 - 00	3.240	0.457
	> 400	0.108	0.703	> 400	0.760	0.215
≥ 65 °	< 20	0.562	0.326	< 50	24.000	1.000
	20 - 500	0.331	0.503	50 - 500	2.800	0.451
	> 500	0.087	0.718	> 500	0.639	0.213

Table 3. Constants for the heat transfer and pressure drop calculation in a PHE with chevron plates [14]

The optimization problem is formulated in such a way that the best combination of the parameters of a given PHE minimizes the number of plates. The optimization method used is based on screening [15], where for a given type of plate, the number of thermal plates is the objective function that has to be minimized. In order to avoid impossible or non-optimal solutions, certain inequality constraints are employed. An algorithm has been proposed in a screening method that uses MATLAB for optimization of a PHE, considering the plate type as the optimization variable [16]. For each type of plate, local optimal configurations are found (if they exist) that employ the fewest plates. Comparison of all the local optima then gives a global optimum.

5. Formulation of the optimization problem

Minimize:

$$N_P = f\left(N_C, P^I, P^{II}, \phi, Y_h, plate\ type\right) \tag{37}$$

Subject to:

$$N_C{}^{min} \le N_C \le N_C{}^{max} \tag{38}$$

$$\Delta P_{hot} \le \Delta P_{hot}{}^{max} \tag{39}$$

$$\Delta P_{cold} \le \Delta P_{cold}{}^{max} \tag{40}$$

$$v_{hot} \ge v_{hot}{}^{min} \tag{41}$$

$$v_{cold} \ge v_{cold}{}^{min} \tag{42}$$

$$E^{min} \le E \le E^{max} \tag{43}$$

If closed-form model is considered, as the closed-form equations are limited for some number of passes, there are two more constraints:

$$P^I \le P^{I,max} \text{ if using closed–form model} \tag{44}$$

$$P^{II} \le P^{II,max} \text{ if using closed–form model} \tag{45}$$

Depending on the equipment model, the number of plates can vary between 3 and 700. The first constraint (38) is imposed according to the PHE capacity. Constraints (39) and (40) can also be imposed, depending on the available pumping power. The velocity constraints are usually imposed in order to avoid dead spaces or air bubbles inside the set of plates. In practice, velocities less than 0.1 m/s are not used [5].

The optimization problem is solved by successively evaluating the constraints, reducing the number of configurations until the optimal set (OS) is found (if it exists). The screening process begins with the identification of an initial set (IS) of possible configurations, considering the channel limits. A reduced set (RS) is generated by considering the velocity and pressure drop constraints. The constraint of thermal effectiveness is then applied to the RS, in increasing order of the number of channels. Configurations with the smallest number of channels form the local optima set. The global optimum can therefore be found by comparing all the local optima. It is important to point out that the global optimum configuration may have a larger total heat transfer area. However, it is usually more economical to use a smaller number of large plates than a greater number of small plates [17]. The optimization algorithm is described in Table 4.

In Step 5, both methods can be used. The model using algebraic equations has the limitation of only being applicable to PHEs that are sufficiently large not to be affected by end channels and channels between adjacent passes. Industrial PHEs generally possess more than 40 thermal plates, although the limitation of the number of passes can still be a drawback. The major advantage of the model using differential equations is its general applicability to any configuration, without having to derive a specific closed-form equation for each configuration.

Steps	Mathematical relations	Comments
Step 1: Input data for each type of plate.		PHE dimensions, fluids physical proprieties, mass flow rate and inlet temperature of both streams, constraints.
Step 2: Verification of the number of plates constraint. The initial set of configurations (IS) is determined.	$\overline{N}_C = N_C{}^{min} : N_C{}^{max}$	The vector $\overline{N}_C$ is generated with all possible number of channels.
Step 2.1: For each element of the vector $\overline{N}_C$, all possible number of passes for sides I and II are computed.	$N_C^I = \dfrac{2N_C + 1 + (-1)^{N_C+1}}{4}$ $N_C^{II} = \dfrac{2N_C - 1 + (-1)^{N_C}}{4}$ $P \leq P^{max}$ if using closed-form model	They are integer divisors of the number of channels of the corresponding side. If one is using closed-form equations, the number of passes constraint must be considered.
Step 3: Verification of the hydraulic constraints. The reduced set of configurations (RS) is determined.	$\Delta P_{fluid} \leq \Delta P_{fluid}{}^{max}$ $v_{fluid} \geq v_{fluid}{}^{min}$	Fluid velocity and pressure drop constrains are verified.
Step 3.1 Take $Y_h = 0$ and check the following constraints.	$P_{cold}^I = P^I$ and $P_{hot}^{II} = P^{II}$.	Cold fluid flows in the side I and the hot fluid in the side II.
Step 3.1.1 Verification of the velocity constraint for the fluid in side I.	$v^I{}_{cold} = \dfrac{G_{C,cold}^I}{\rho_{cold}}$	Cold fluid velocity $v^I{}_{cold}$ is calculated, in a decreasing order of the possible number of passes of a given element of $\overline{N}_C$. If $v^I{}_{cold}$ achieves the minimum

Steps	Mathematical relations	Comments
		allowable value, it is not necessary to evaluate configurations with smaller number of passes.
Step 3.1.2 Verification of the pressure drop constraint in side I	Eq. (31)	The cold fluid pressure drop is calculated, ΔP^{I}_{cold} , in a crescent order of the possible number of passes of a given element of $\overline{N}_C$. If ΔP^{I}_{cold} achieves the maximum allowable value, it is not necessary to evaluate configurations with greater number of passes.
Step 3.1.3 Verification of the velocity constraint for the fluid in side II.	$v^{II}_{hot} = \dfrac{G^{II}_{C,hot}}{\rho_{hot}}$	Analogous to Step 3.1.1.
Step 3.1.4 Verification of the pressure drop constraint in side II.	Eq. (31)	Analogous to Step 3.1.2.
Stage 3.2 Take Y_h =1 and do the same as Stage 3.1.	$P^{II}_{cold} = P^{II}$ and $P^{I}_{hot} = P^{I}$.	Analogous to stage 3.1.
Stage 3.3: Combination of the configuration parameters.	$[N_C P^I P^{II} Y_h \phi]$	For Y_h = 0 and Y_h =1 , the number of passes selected for the sides I and II of the PHE is combined.
Step 4: Calculate the effectiveness in pure countercurrent flow, E_{CC}.	$E_{CC} = \begin{cases} \dfrac{1-e^{-NTU(1-C_r)}}{1-C_r e^{-NTU(1-C_r)}} if \ C_r < 1 \\[2em] \dfrac{NTU}{NTU+1} if \ C_r = 1 \end{cases}$	If $E_{CC} < E^{min}$, these configurations can be discarded.
Step 5: Verification of the thermal effectiveness constraint. The local optimal set of configurations (OS) is determined.	$E^{min} \le E \le E^{max}$	The selected configurations in Step 4 are simulated in a crescent order of the number of channels to find the possible local optimum set (OS). The remaining configurations do not need to be simulated. Both modeling can be used.
Step 6: Find global optimum.		By comparing all local optima, the global optimum is found.

Table 4. Optimization algorithm.

However, a drawback is the highly complex implementation of the simulation algorithm (see Table 5), in contrast to the second model, which is very simple.

Steps	Equations and tables	Comments
Step 1. Tri-diagonal matrix coefficients are computed.	$d_{(i)} = s_{(i)}\alpha^{(I \, or \, II)}$ and Table 7	As $s_{(i)}$ depends on the configuration of the PHE, it can be calculated by means of an algorithm.
Step 2. Tri-diagonal matrix construction.	Eq. (6)	
Step 3. Eigenvalues and eigenvectors are computed.		If one is using Matlab, one can use build-in functions.
Step 4. Linear system generation.	$\overline{\overline{A}}.\overline{C} = \overline{B}$ and Table 6	The boundary condition equations in algorithmic form of inlet fluids and change of pass are used.
Step 4.1. Generation of eigenvalues and eigenvectors matrix, $\overline{\overline{A}}$, and the binary vector, $\overline{B}^I$.	$\overline{\overline{A}} = \overline{\overline{A}}^{\,I} + \overline{\overline{A}}^{\,II}$ $\overline{B} = \overline{B}^I + \overline{B}^{II}$	The resulting matrices are the sum of the matrices of both sides of the PHE.
Step 5. Determination of c_i's coefficients by solving the linear system.	$\overline{C} = \overline{B} * \overline{\overline{A}}^{-1}$	
Step 6. Determination of the output dimensionless temperatures.	Table 6	The boundary condition of output fluid in algorithmic form is used.
Step 7. Computation of thermal effectiveness.	$E = \begin{cases} E^I = \dfrac{N^I}{\alpha^I} max\left(\dfrac{\alpha^I}{N^I}, \dfrac{\alpha^{II}}{N^{II}}\right) \mid \theta_{in} - \theta_{out} \mid^I \\ E^{II} = \dfrac{N^{II}}{\alpha^{II}} max\left(\dfrac{\alpha^I}{N^I}, \dfrac{\alpha^{II}}{N^{II}}\right) \mid \theta_{in} - \theta_{out} \mid^{II} \end{cases}$	It may be obtained considering any side of the PHE, because the energy conservation is obeyed only if $E = E^I = E^{II}$.

Table 5. Simulation algorithm.

5.1. Simulation algorithm for the model using differential equations

For the development of this algorithm, the boundary conditions equations are used in the algorithm form described previously [6] (see Table 6). The simulation algorithm is applied separately for each value of ϕ separately. The algorithm is presented below.

6. Case study

A case study was used to test the developed algorithm and compare the two mathematical models. Data were taken from examples presented in [18]. A cold water stream exchanges heat with a hot water stream of process. As the closed-form equations only consider configurations with a maximum of 4 passes for each fluid, a case was chosen in which the reduced set only had configurations with less than 4 passes for each stream. Table 8 presents the data used. Only one type of plate was considered.

The RS was obtained by applying the optimization algorithm up to Step 3. The optimal set was found by applying Step 5. As only one type of plate was considered, the local optimum was

also the global optimum. The same optimal set was found with both approaches: two heat exchanger configurations with 144 channels and a 3-2 asymmetric pass arrangement (as presented in Table 9).

	Fluid inlet	Fluid outlet
Boundary conditions for side I.	For $n = 1$ to $n = N^I$ $\quad \theta_{2n-1}(\eta = 0) = \theta_{in}{}^I$ end	$\theta_{out}{}^I = \dfrac{1}{N^I} \displaystyle\sum_{i=1}^{N^I} \theta_{2(P^I-1)N^I+2i-1}\left(\eta = \dfrac{(-1)^{P^I+1}+1}{2}\right)$
	Change of pass	
	for $p = 2$ to $p = P^I$ $\quad$ for $n = 1$ to $n = N^I$ $\qquad \theta_{2(p-1)N^I+2n-1}\left(\eta = \dfrac{(-1)^p+1}{2}\right) = \dfrac{1}{N^I}\displaystyle\sum_{i=1}^{N^I}\theta_{2(p-2)N^I+2i-1}\left(\eta = \dfrac{(-1)^p+1}{2}\right)$ $\quad$ end end	
	Fluid inlet	**Fluid outlet**
Boundary conditions for side II ($\phi = 1$).	for $n = 1$ to $n = N^I$ $\quad \theta_{2n}(\eta = 0) = \theta_{in}{}^{II}$ end	$\theta_{out}{}^{II} = \dfrac{1}{N^{II}} \displaystyle\sum_{i=1}^{N^{II}} \theta_{2(P^{II}-1)N^{II}+2i}\left(\eta = \dfrac{(-1)^{P^{II}+1}+1}{2}\right)$
	Change of pass	
	for $p = 2$ to $p = P^I$ $\quad$ for $n = 1$ to $n = N^I$ $\qquad \theta_{2(p-1)N^{II}+2n}\left(\eta = \dfrac{(-1)^p+1}{2}\right) = \dfrac{1}{N^{II}}\displaystyle\sum_{i=1}^{N^{II}}\theta_{2(p-2)N^{II}+2i}\left(\eta = \dfrac{(-1)^p+1}{2}\right)$ $\quad$ end end	
	Fluid inlet	**Fluid outlet**
Boundary conditions for side II ($\phi = 2$).	for $n = 1$ to $n = N^I$ $\quad \theta_{2n}(\eta = 1) = \theta_{in}{}^{II}$ end	$\theta_{out}{}^{II} = \dfrac{1}{N^{II}} \displaystyle\sum_{i=1}^{N^{II}} \theta_{2(P^{II}-1)N^{II}+2i}\left(\eta = \dfrac{(-1)^{P^{II}}+1}{2}\right)$
	Change of pass	
	for $p = 2$ to $p = P^I$ $\quad$ for $n = 1$ to $n = N^I$ $\qquad \theta_{2(p-1)N^{II}+2n}\left(\eta = \dfrac{(-1)^{p+1}+1}{2}\right) = \dfrac{1}{N^{II}}\displaystyle\sum_{i=1}^{N^{II}}\theta_{2(p-2)N^{II}+2i}\left(\eta = \dfrac{(-1)^{p+1}+1}{2}\right)$ $\quad$ end end	
	Fluid inlet	**Fluid outlet**
Boundary conditions for side II ($\phi = 3$).	for $n = 1$ to $n = N^I$ $\quad \theta_{2(P^{II}-1)N^{II}+2n}(\eta = 0) = \theta_{in}{}^{II}$ end	$\theta_{out}{}^{II} = \dfrac{1}{N^{II}} \displaystyle\sum_{i=1}^{N^{II}} \theta_{2i}\left(\eta = \dfrac{(-1)^{P^{II}+1}+1}{2}\right)$
	Change of pass	
	for $p = 2$ to $p = P^I$ $\quad$ for $n = 1$ to $n = N^I$ $\qquad \theta_{2(p-2)N^{II}+2n}\left(\eta = \dfrac{(-1)^{P^{II}+p}+1}{2}\right) = \dfrac{1}{N^{II}}\displaystyle\sum_{i=1}^{N^{II}}\theta_{2(p-1)N^{II}+2i}\left(\eta = \dfrac{(-1)^{P^{II}+p}+1}{2}\right)$ $\quad$ end end	
	Fluid inlet	**Fluid outlet**
Boundary conditions for side II ($\phi = 4$).	for $n = 1$ até $n = N^I$ $\quad \theta_{2(P^{II}-1)N^{II}+2n}(\eta = 1) = \theta_{in}{}^{II}$ end	$\theta_{out}{}^{II} = \dfrac{1}{N^{II}} \displaystyle\sum_{i=1}^{N^{II}} \theta_{2i}\left(\eta = \dfrac{(-1)^{P^{II}}+1}{2}\right)$
	Change of pass	
	for $p = 2$ to $p = P^I$ $\quad$ for $n = 1$ to $n = N^I$ $\qquad \theta_{2(p-2)N^{II}+2n}\left(\eta = \dfrac{(-1)^{P^{II}+p+1}+1}{2}\right) = \dfrac{1}{N^{II}}\displaystyle\sum_{i=1}^{N^{II}}\theta_{2(p-1)N^{II}+2i}\left(\eta = \dfrac{(-1)^{P^{II}+p+1}+1}{2}\right)$ $\quad$ end end	

Table 6. Boundary conditions [6].

Side I	for $p = 2$ to $p = P^I$ $\quad$ for $n = 1$ to $n = N^I$ $\qquad i = 2(p-1)N^I + 2n - 1$ $\qquad s_i = (-1)^{p+1}$ $\quad$ end end
Side II	for $p = 2$ to $p = P^I$ $\quad$ for $n = 1$ to $n = N^I$ $\qquad i = 2(p-1)N^I + 2n - 1$ $\qquad$ if $\phi = 1$: $s_i = (-1)^{p+1}$ $\qquad$ if $\phi = 1$: $s_i = (-1)^{p}$ $\qquad$ if $\phi = 1$: $s_i = (-1)^{P^{II}+p}$ $\qquad$ if $\phi = 1$: $s_i = (-1)^{P^{II}+p+1}$ $\quad$ end end

Table 7. Algorithm to define the flow direction [6].

Plate characteristics	
$L_P = 1.38$ m	$\beta = 50\,°$
$W_P = 0.535$ m	$\Phi = 1.15$
$b = 3.7$ mm	$t_P = 0.6$ mm
$D_P = 150$ mm	$k_P = 17$ W/m·K
Process-water	**Cooling-water**
$T_{in,hot} = 87.0\,°C$	$T_{in,cold} = 20.0\,°C$
$\dot{M}_{hot} = 26.0$ kg/s	$\dot{M}_{cold} = 62.5$ kg/s
Constraints	
$80 \leq N_C \leq 150$	$E^{min} = 90\%$
$10 \leq \Delta P_{hot} \leq 20$ psi	$0 \leq \Delta P_{cold} \leq 25$ psi
$v_{hot}{}^{min} = 0.0$ m/s	$v_{cold}{}^{min} = 0.6$ m/s

Table 8. Example data

It can be seen from the Tables that the simulations using the two models resulted in values that were very close. It is important to point out that the closed-form equations are only applicable when the end effects can be neglected (in the present case, when the number of thermal plates was greater than 40).

#	N_C	P^I	P^{II}	Y_h	E (differential equation model)				E (closed-form model)			
					$\phi=1$	$\phi=2$	$\phi=3$	$\phi=4$	$\phi=1$	$\phi=2$	$\phi=3$	$\phi=4$
1	80	1	2	0	80.1	80.3	80.3	80.1	80.4	80.4	80.4	80.4
2	80	2	1	1	80.3	80.1	80.3	80.1	80.4	80.4	80.4	80.4
3	81	1	2	0	80.3	80.3	80.3	80.3	80.6	80.6	80.6	80.6
4	83	2	1	1	80.5	80.5	80.5	80.5	80.8	80.8	80.8	80.8
5	84	1	2	0	80.5	80.8	80.8	80.5	80.9	80.9	80.9	80.9
6	84	2	1	1	80.8	80.5	80.8	80.5	80.9	80.9	80.9	80.9
7	85	1	2	0	80.8	80.8	80.8	80.8	81.0	81.0	81.0	81.0
8	87	2	1	1	80.9	80.9	80.9	80.9	81.2	81.2	81.2	81.2
9	88	1	2	0	80.9	81.2	81.2	80.9	81.3	81.3	81.3	81.3
10	88	2	1	1	81.2	80.9	81.2	80.9	81.3	81.3	81.3	81.3
11	89	1	2	0	81.2	81.2	81.2	81.2	81.4	81.4	81.4	81.4
12	91	2	1	1	81.4	81.4	81.4	81.4	81.6	81.6	81.6	81.6
13	92	1	2	0	81.3	81.6	81.6	81.3	81.7	81.7	81.7	81.7
14	92	2	1	1	81.6	81.3	81.6	81.3	81.7	81.7	81.7	81.7
15	93	1	2	0	81.6	81.6	81.6	81.6	81.8	81.8	81.8	81.8
16	95	2	1	1	81.7	81.7	81.7	81.7	82.0	82.0	82.0	82.0
17	96	1	2	0	81.7	81.9	81.9	81.7	82.1	82.1	82.1	82.1
18	96	2	1	1	81.9	81.7	81.9	81.7	82.1	82.1	82.1	82.1
19	97	1	2	0	81.9	81.9	81.9	81.9	82.2	82.2	82.2	82.2
20	144	2	3	0	71.8	71.7	92.8	92.9	71.8	71.8	93.0	93.0
21	144	3	2	1	71.7	71.8	92.8	92.9	71.8	71.8	93.0	93.0
22	149	3	2	1	71.7	71.7	93.0	93.0	71.7	71.7	93.2	93.2

■ Optimal configurations

Table 9. Thermal effectiveness of RS for both mathematical models

7. Conclusions

In this chapter it was presented the development of two models for the design and optimization of plate heat exchangers. Both mathematical models were used to accomplish the heat exchanger design simulations. These methods use differential equations and closed-form equations based on the notion that a multi-pass PHE can be reduced to an arrangement consisting of assemblies of single-pass PHEs.

As a case study, an example obtained from the literature was used. The optimal sets were the same for both approaches, and agreement was achieved between the effectiveness values. The model using algebraic equations has the limitation of only being applicable to PHEs sufficiently large not to be affected by end channels and channels between adjacent passes. However, industrial PHEs generally possess more than 40 thermal plates. The major advantage of using this model is its general applicability to any configuration, without having to derive a specific closed-form equation for each configuration. However, its drawback is the highly complex implementation of the simulation algorithm, unlike the second approach, which is very simple.

Nomenclature

A	Effective plate heat transfer area (m^2)
A_p	Plate effective area, m^2
$\bar{\bar{A}}$	Eigenvalues and eigenvectors matrix
b	Average thickness channel, m
$\bar{B}$	Binary vector
c_p	Specific heat, J/kg·K
C_r	Heat capacity ratio
$\bar{C}$	c_i coefficients vector
D_e	Equivalent diameter of the channel(m)
D_p	Port diameter of the plate(m)
E	Exchanger effectiveness, %
E_{CC}	Thermal effectiveness in purely countercurrent flow (%)
f	Fanning factor
g	Gravitational acceleration (m/s^2)
G_C	Channel mass velocity (kg/m^{2}s)
G_P	Port mass velocity (kg/m^{2}s)
IS	Initial set of configurations
k	Thermal conductivity(W/mK)
k_P	Plate thermal conductivity, W/m·K
L_P	Plate length, m
L_H	Horizontal port distance (m)
L_V	Vertical port distance (m)

$\dot{m}$	mass velocity per channel (kg/s)
$\dot{M}$	Mass flow rate, kg/s
$\bar{\bar{M}}$	Tri-diagonal matrix
N	Number of channels per pass
N_C	Number of channels
N_P	Number of plates
NTU	Number of transfer units
Nu	Nusselt number
OS	Optimal set of configurations
P	Number of passes
P_C	Temperature effectiveness
Pr	Prandtl number
Q	Heat transfer rate(J/s)
R	Heat capacity rate ratio
R_f	Fouling factor, K/W
Re	Reynolds number
RS	Reduced set of configurations
s_i	Binary parameter for flow direction
t_P	Plate thickness, m
U	Overall heat transfer coefficient, W/m²·K
v	Fluid velocity inside channels, m/s
W_P	Plate width, m
Y_h	Binary parameter for hot fluid location
Y_f	Binary parameter for type of channel flow
z_i	Eigenvector of the tri-diagonal matrix

Greek symbols

α	Heat transfer coefficient
β	Chevron corrugation inclination angle, degrees
ΔP	Pressure drop, Pa
ΔT_{lm}	Log-mean temperature difference (K)

ΔT_M	Effective mean temperature difference (K)
η	Normalized plate length
θ	Dimensionless fluid temperature
λ	Eingevalue of the tri-diagonal matrix
μ	viscosity (Pa.s)
μ_w	Viscosity at wall temperature (Pa.s)
ρ	density (kg/m³)
Φ	Enlargement factor of the plate area
ϕ	Parameter for feed connections position

Subscripts

cold	Cold fluid
CC	Countercurrent
hot	Hot fluid
i	Generic element
in	Inlet
j	Generic element
out	Outlet

Superscripts

I	Odd channels of the heat exchanger
II	Even channels of the heat exchanger
max	Maximum
min	Minimum

Author details

Fábio A.S. Mota[1,2], E.P. Carvalho[2] and Mauro A.S.S. Ravagnani[2*]

*Address all correspondence to: ravag@deq.uem.br

1 National Institute for Space Research, São José dos Campos, SP, Brazil

2 Chemical Engineering Graduate Program - State University of Maringá, Maringá, PR, Brazil

References

[1] Alfa Laval. Canada. Plate Heat Exchanger: A Product Catalogue for Comfort Heating and Cooling. Available in <http://www. pagincorporated.com>. (Accessed 20 October 2010).

[2] Sondex. Louisville. Plate Type Heat Exchangers: Operation & Maintenance Manual. Availble in <http://www.sondex-usa.com>. (Accessed 26April 2011).

[3] Shah, R. K.; Sekulic, D. P. Fundamentals of Heat Exchanger Design. New Jersey: John Wiley & Sons, Inc. 2003. Page 24.

[4] Taco. Craston. Plate Heat Exchanger: Operational and Maintenance Manual. Available in <http://www. taco-hvac.com>. (Accessed 18 May 2011).

[5] Kakaç S., Liu H., Heat Exchanger: Selection, Rating and Thermal Design, 2ed. Boca Raton: CRC Press, 2002.

[6] J. A. W. Gut, J. M Pinto, Modeling of Plate Heat Exchangers with Generalized Configurations. Int. J. Heat Mass Transfer 2003; 46:2571-2585.

[7] Kho, T. Effect of Flow Distribution on Scale Formation in Plate Heat Exchangers. Thesis (PhD) – University of Surrey, Surrey, UK, 1998.

[8] Wang L., Sundén B., Manglik R. M., *Plate Heat Exchangers: Design, Applications and Performance*, Ashurst Lodge: WIT Press, 2007, pp. 27-39.

[9] Alfa Laval. Canada. Plate Heat Exchanger: Operational and Maintenance Manual. Available in <http://www. schaufcompany.com>. Accessed: 18 May 2011.

[10] Lienhard IV, J. H.; Lienhard V, J. H. A Heat Transfer Textbook. 3ed. Cambridge: Phlogiston Press, 2004. Page 103.

[11] Kandlikar, S. G.; Shah, R.K. Asymptotic Effectiveness-NTU Formulas for Multipass Plate Heat Exchangers. Journal of Heat Transfer, v.111, p.314-321, 1989.

[12] Heggs, P. J. e Scheidat, H. J. Thermal Performance of Plate Heat Exchangers with Flow Maldistribution. Compact Heat Exchangers for Power and Process Industries, ed. R. K. Shah, T. M. Rudy, J. M. Robertson, e K. M. Hostetler, HTD, vol.201, ASME, New York, p.621-626, 1996.

[13] Shah, R. K.; Kandlikar, S. G. The Influence of the Number of Thermal Plates on Plate Heat Exchanger Performance. In: MURTHY, M.V.K. et al. (Ed.) Current Research in Heat and Mass Transfer. New York: HemisTCPre P.C., 1988, p.227-241.

[14] Kumar, H. The Plate Heat Exchanger: Construction and Design. 1st UK National Conference of Heat Transfer. n.86, p.1275-1286, 1984.

[15] Gut J. A. W., Pinto J. M, Optimal Configuration Design for Plate Heat Exchangers. Int. J. Heat Mass Transfer 2004; 47:4833-4848.

[16] Mota F. A. S., Ravagnani M. A. S. S., Carvalho E. P., Optimal Design of Plate Heat Exchangers. Applied Thermal Enginnering 2014;63:33-39. 2013.

[17] Hewitt, G. F.; Shires, G.L.; Bott, T.R. Process Heat Transfer. Boca Raton: CRC Press, 1994.

[18] Gut, J. A. W.; Configurações Ótimas de Trocadores de Calor a Placas. 2003. 244p. Tese (Doutorado) – Escola Politécnica, Universidade de São Paulo, São Paulo, 2003.